

Metal–Insulator Transition in 2D: Experimental Test of the Two-Parameter Scaling

D. A. Knyazev¹, O. E. Omel'yanovskii¹, V. M. Pudalov¹, I. S. Burmistrov^{2,3}

¹*P. N. Lebedev Physical Institute RAS, 119991 Moscow, Russia*

²*L.D. Landau Institute for Theoretical Physics RAS, Kosygina street 2, 119334 Moscow, Russia and*

³*Department of Theoretical Physics, Moscow Institute of Physics and Technology, 141700 Moscow, Russia*

(Dated: February 12, 2008)

We report a detailed scaling analysis of resistivity $\rho(T, n)$ measured for several high-mobility 2D electron systems in the vicinity of the 2D metal-insulator transition. We analyzed the data using the two parameter scaling approach and general scaling ideas. This enables us to determine the critical electron density, two critical indices, and temperature dependence for the separatrix in the self-consistent manner. In addition, we reconstruct the empirical scaling function describing a two-parameter surface which fits well the $\rho(T, n)$ data.

PACS numbers: 71.30.+h, 73.43.Nq, 71.27.+a

The experimental discovery [1, 2, 3] of the metal-insulator transition (MIT) in the two-dimensional (2D) electron system of high mobility silicon metal-oxide-semiconductor (Si-MOS) field-effect transistors still calls for a theoretical explanation. Perhaps, the most promising framework is provided by the microscopic theory, initially developed by Finkelstein, which combines disorder and strong electron–electron (e - e) interaction [4]. Recently, Punnoose and Finkelstein [5] have shown the possibility of the MIT for a special model of the 2D electron system with the infinite number of valleys. The key feature of the theory is the existence of the *two-parameter scaling* near the criticality. One scaling variable is governed by disorder, and the other is determined by e - e interaction. In accord with the theoretical prediction, the renormalization of both resistivity and e - e interaction with temperature has been experimentally demonstrated [6, 7].

The main objective of the present Letter is to test experimentally the two-parameter scaling. We present our results for the detailed analysis of the temperature (T) and electron density (n) dependence of resistivity (ρ) measured on five Si-MOS samples. From this analysis, we identify the two scaling variables together with the corresponding exponents (see Table I) and determine for the first time the scaling function for resistivity in the metallic region in the vicinity of the MIT. We have found that the two-parameter scaling provides a natural explanation for the following set of experimental observations in the vicinity of the MIT: (i) the separatrix, $\rho_c(T) \equiv \rho(T, n_c)$, has a monotonic power-law temperature dependence, where n_c denotes the critical density; (ii) a generic $\rho(T, n)$ curve on the metallic side ($n > n_c$) is nonmonotonic in T , and has a maximum and an inflection point; (iii) for $n = n_c$, the maximum and inflection points merge at zero temperature; (iv) the normalized $\rho(T, n)/\rho_c(T)$ data in the vicinity of the MIT obey the mirror reflection symmetry that is fulfilled in much wider ranges of $n - n_c$ and T , as compared to the symmetry previously reported under the assumption of the

T -independent separatrix [8].

For the measurements we have selected five representative Si-MOS samples of the rectangular geometry from four different (001)-Si wafers. Their peak mobilities are listed in Table I. We have used four-terminal ac-technique at the 5 Hz frequency. The source–drain current was chosen low enough, e.g., $I = 10$ nA for $T = 1.3$ K, in order to avoid electron overheating. Most of studies were performed in the range 1.3 – 4.2 K, because for these temperatures (i) the critical region of densities $|\Delta n| = |n - n_c|$ becomes sufficiently wide as will be shown below, and (ii) $\rho(T)$ near the criticality exhibits a well-pronounced maximum (Fig. 1), which provides an additional tool for comparison with the theory. For two samples, Si15 and Si62, we have performed the measurements down to 0.3 K; for sample Si43, we have extended the temperature range up to 1 – 38 K in order to illuminate the overall trend of the resistivity maximum and the scaling behavior of $\rho(T, n)$.

Figure 1 shows a typical $\rho(T)$ -dependence for two samples, Si2 (Si43), in the critical regime, in the density range from 0.672 to 1.12 (0.707 to 1.49), in units of 10^{11} cm^{-2} [9]. As n decreases, the $\rho(T)$ behavior crosses over from metallic ($n > n_c$) to insulating ($n < n_c$) one. Initially and during about a decade [2, 3, 8], the data were analyzed within the framework of the one-parameter scaling (OPS) theory, in which n is a single driving parameter. Within this approach the separatrix $\rho_c(T)$ separating the metallic from insulating domains should be T -independent, i.e., $\rho_c(T) = \rho_0$. As a result, in the vicinity of n_c , the $\rho(T, n)$ data should obey the reflection symmetry [11]: $\rho(T, n_c - \Delta n) = \rho_0^2/\rho(T, n_c + \Delta n)$ when $\Delta n \ll n_c$. This obviously disagrees with the data shown in Fig. 1, i.e., the OPS theory cannot adequately describe the data within the whole T -range. In view of this well-known problem [12], it is a common practice to use the OPS approach for the analysis of the data in a *truncated* temperature range.

In theory [4], physics at $T = 0$ is described by the two coupled renormalization group (RG) equations for

conductance σ (in units e^2/h) and interaction amplitude $\gamma_2 = -F_0^\sigma/(1 + F_0^\sigma)$ where F_0^σ denotes the standard Fermi-liquid parameter in the triplet channel [4, 13]:

$$\frac{d\sigma}{d\eta} = \beta_\sigma(\sigma, \gamma_2), \quad \frac{d\gamma_2}{d\eta} = \beta_{\gamma_2}(\sigma, \gamma_2). \quad (1)$$

Here $\eta = \ln L/l$, L stands for the running RG length-scale (sample size), and l is the microscopic lengthscale (elastic mean free path), at which the RG starts. In the microscopic theory [4], the temperature appears as Tz which has a dimensionality of L^{-2} , and the parameter z varies with L according to $d \ln z / d\eta = \gamma_z(\sigma, \gamma_2)$. The RG equations should be supplemented with the initial conditions at $\eta = 0$: $\sigma(0) = \bar{\sigma}$, $\gamma_2(0) = \bar{\gamma}_2$, and $z(0) = \bar{z}$, where $\bar{\sigma}, \bar{\gamma}_2$ and \bar{z} are sample dependent. Following the scaling ideas [14], we expect the measured resistivity $\rho = \rho(T\bar{z}, \bar{\sigma}, \bar{\gamma}_2, l)$ to be independent of microscopic details: $d\rho/dl = 0$. Applying the standard analysis of the Callan-Symanzik equation [14], we find that the measured resistance is a function of two scaling variables X and Y , $\rho = \mathcal{R}(X, Y)$, where \mathcal{R} is a regular function.

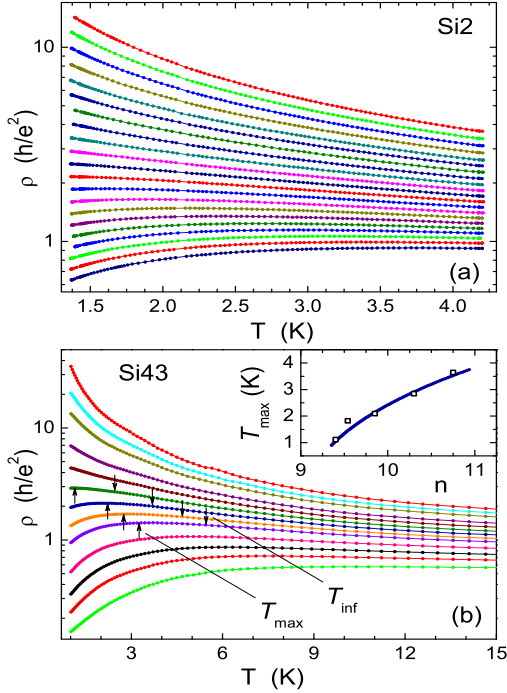


FIG. 1: Temperature dependences $\rho(T)$: (a) for sample Si2; the densities increase in steps of 0.224 starting from 6.72 (top-most curve). (b) for sample Si43; the densities are (from top to bottom) 7.16, 7.34, 7.52, 7.70, 7.88, 8.06, 8.51, 8.96, 9.41, 9.86, 10.31, 10.76, 11.6, 12.5, 13.4, 14.9. The inset shows T_{\max} vs electron density: squares are the data, and line is the theoretical curve (see below). Density values are quoted in units of 10^{10} cm^{-2} .

The MIT implies the existence of a fixed point (FP) determined by the conditions: $\beta_\sigma(\sigma^c, \gamma_2^c) = \beta_{\gamma_2}(\sigma^c, \gamma_2^c) =$

0. Linearizing Eqs. (1) near the fixed point, one finds

$$X = (T/T_0)^{-\kappa}(n - n_c)/n_c, \quad Y = (T/T_1)^\zeta. \quad (2)$$

Here $\kappa = p/(2\nu)$ and $\zeta = -py/2$, where the correlation length exponent ν and the irrelevant exponent $y < 0$ are given by the eigenvalues of the linearized Eqs. (1) [14]. The exponent $p = 2/[2 + \gamma_z(\sigma^c, \gamma_2^c)]$ governs the T -behavior of the specific heat at the fixed point; $T_{0,1}$ are sample-dependent energy scales. Temperature T_0 corresponds to the bandwidth of the available states participating in the transport and is of the order of the elastic scattering rate $\hbar/2k_B\tau$. Temperature T_1 determines the quantum critical region at $n = n_c$ [15]. Deriving Eq. (2), we expressed $\bar{\sigma}$ and $\bar{\gamma}_2$ in terms of the experimentally measurable parameters μ and n .

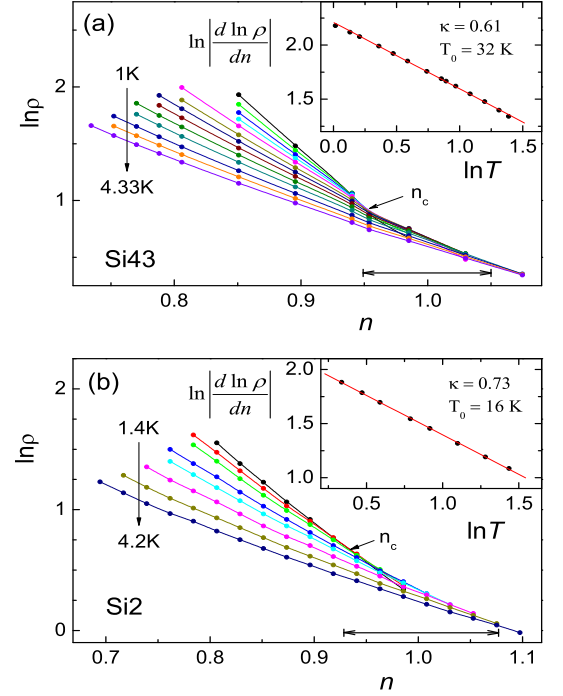


FIG. 2: The density dependences of $\ln \rho(n)$ for various temperatures (from the top to the bottom, in K): (a) 1, 1.23, 1.43, 1.6, 1.8, 2.1, 2.35, 2.64, 2.95, 3.31, 3.71, 4, 4.33 for sample Si43, (b) 1.4, 1.6, 1.8, 2.2, 2.5, 3, 3.6, 4.2 for sample Si2. The density is given in units of 10^{11} cm^{-2} . The data are shown in a limited density range, $X < 0.7$. The insets illustrate the procedure of extracting κ and T_0 using Eq. (3). The bars display the range of intersections for all curves.

At present, the explicit form of $\mathcal{R}(X, Y)$ is unknown. In general, even in the vicinity of the FP, X and Y are not necessarily small. However, from the common-sense arguments we require that at $T \rightarrow 0$ the system (i) is an insulator for $n < n_c$, i.e., $\mathcal{R}(-\infty, 0) = \infty$; (ii) is a metal for $n > n_c$, i.e., $\mathcal{R}(+\infty, 0) = 0$; and (iii) is at the quantum critical point for $n = n_c$, i.e., $\mathcal{R}(0, 0) = \rho_c^0$. Following arguments of Ref. [11], we assume that

$$\rho(T, n) = \mathcal{R}(X, Y) = \rho_c^0 e^{-X} (1 - Y), \quad |X|, Y \ll 1. \quad (3)$$

This is consistent with all the requirements listed above. In particular, such a form of $\mathcal{R}(X, Y)$ provides the reflection symmetry for the normalized resistance $\rho(T)/\rho_c(T)$.

In the vicinity of n_c , on the metallic side, $n > n_c$, the $\rho(T, n)$ data exhibit a maximum at a certain density-dependent temperature T_{\max} (see Fig. 1). The inset to Fig. 1 shows that T_{\max} vanishes as $n \rightarrow n_c$, in agreement with Eq. (3), which predicts a monotonic $\rho_c(T)$ dependence. On the insulating side, for n lower but close to n_c , the $\rho(T, n)$ curves have a positive curvature. Therefore, the neighboring curves on the metallic side should also have a positive curvature at sufficiently high temperatures. This expectation agrees with the experiment (Fig. 1). It follows from the above results that each of the nonmonotonic $\rho(T, n)$ curves must have an *inflection point*. Its existence restricts the exponent ζ to be less or equal to unity, $\zeta \leq 1$. As a result, not only T_{\max} but also the inflection point temperature T_{\inf} vanish at $n = n_c$.

In order to test the theoretical prediction, we have adopted a procedure employed for studying the scaling behavior near the criticality in the quantum Hall regime [15]. We plot in Fig. 2 the $\ln \rho(T, n)$ data for various temperatures versus n for $X \lesssim 1$. Two features are clearly seen in Fig. 2. Firstly, as T decreases, the region of intersection for the $\ln \rho(T, n)$ curves shrinks. This enables one to determine an approximate n_c value as an intersection point in the $T = 0$ limit. Secondly, in the vicinity of n_c (for small X), the $\ln \rho(T, n)$ curves are linear in n in accordance with Eq. (3). In the insets to Fig. 2, we plot the logarithmic slopes of the $\ln \rho(T, n)$ curves versus $\ln T$. The resulting curves appear to be linear; this allows us to extract both κ and T_0 values for the five studied samples. The results are summarized in Table I.

Equation (3) predicts that, for $X \ll 1$, the $\rho(T, n)$ data normalized by $\exp(-X)$ should collapse onto a single curve. In order to test this theoretical prediction, we plot the normalized $\rho^*(T) \equiv \rho(T, n) \exp(X)$ data in Fig. 3. We stress that no adjustable parameters are used in this scaling procedure. The critical density n_c , and the T_0 and κ values were determined at the previous stage. As is shown in Fig. 3, the normalized $\rho^*(T)$ data do scale with high accuracy, 0.8%, on the $\rho(T, n_c)$ curve in the range $X < 0.5$. The deterioration of the scaling quality for greater X values limits the range of temperatures and densities used for the scaling procedure (Fig. 3). Provided that Eq. (3) adequately describes the separatrix $\rho(T, n_c)$, the scaling procedure enables us to determine the critical n_c value more precisely. For this purpose, we require the low temperature region ($Y \ll 1$) of the scaled curves to have the curvature of the constant sign over the whole temperature range. Indeed, we found that, by adjusting the preliminary determined n_c value within only 2%, the inflection point in the $\rho(T, n_c)$ -data could be easily eliminated for all five samples.

The bunch of the scaled curves in Fig. 3 is fitted with

the theoretical expression (3) for the separatrix $\rho(T, n_c)$, by using the remaining scaling parameters ζ , T_1 and ρ_c^0 as adjustable parameters. The result of fitting for sample Si2 is shown in the inset to Fig. 3. The values of the above parameters extracted from the best fit are given in Table I for all of the five samples. The validity of Eq. (3)

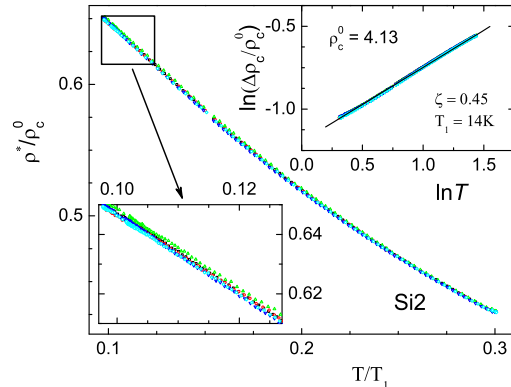


FIG. 3: Scaling of the $\rho^*(T)/\rho_c^0$ data for densities $n = 8.74, 8.96, 9.18, 9.41, 9.63 \times 10^{10} \text{ cm}^{-2}$. The lower inset demonstrates the quality of the scaling for large $X \sim 0.5$. The upper inset shows a fit of the separatrix using Eq. (3) with three parameters ζ , T_1 and ρ_c^0 . Sample Si2

is further supported by the nonmonotonic temperature behavior of $\rho(T, n)$ (Fig. 1). Using the extracted scaling parameters (Table I), we can readily find $T_{\max}(n)$ dependences from Eq. (3). The results are in a good agreement with the experimental data for all of the five samples. A typical example of comparison is shown in the inset to Fig. 1. We note that the data are processed only for $T \leq (4 - 5) \text{ K}$ to ensure the applicability of Eq. (3).

TABLE I: The relevant parameters for the studied samples. μ_{peak} [m^2/Vs] is the peak mobility at $T = 0.3 \text{ K}$, ρ_c^0 is in units of h/e^2 , T_0 and T_1 are in K, and n_c is in 10^{11} cm^{-2} . The inverse transport scattering time $\hbar/2k_B\tau$ [K] is estimated from $\rho_c(T = 4.2 \text{ K})$. The errors for T_0 , κ , n_c are about 2%; the errors for T_1 , ζ , and ρ_c^0 are given in the last column.

sample	μ_{peak}	$\hbar/2k_B\tau$	n_c	T_0	T_1	κ	ζ	ρ_c^0	%
Si15	4.1	13	0.86	12	15	0.82	0.35	4.17	30
Si62	3.6	26	0.94	22	11	0.74	0.5	5.27	20
Si2	3.4	22	0.89	16	14	0.73	0.45	4.13	12
Si43	2.0	31	0.92	32	13.5	0.61	0.8	4.14	12
Si6-14	1.9	26	1.22	26	15	0.66	0.86	2.35	6

Table I shows that the extracted T_0 and T_1 agrees reasonably with $\hbar/2k_B\tau$. In the theory, the exponents κ , and ζ , and the ρ_c^0 value should be universal. Experimentally, there is a trend of κ and ζ^{-1} towards smaller values with decreasing sample mobility. The trend is rather likely to be due to the presence of the long-range components of the random potential for the high mobility Si-MOS samples. This favors a percolation-type behavior to dominate

over the true scaling one [16]. We mention that variation of exponent κ with a sample mobility has recently been observed in the plateau–plateau transitions of the quantum Hall regime [17]. Yet another possible reason that may complicate the scaling analysis of experimental data is an inhomogeneity of the electron density [18].

In contrast to the one-parameter scaling, in the two-parameter case the data should be described by a universal scaling function $\mathcal{R}(X, Y)$, which represents a 2D surface in the (X, Y, ρ) space. Using six parameters determined experimentally, $n_c, \kappa, \zeta, T_{0,1}$ and ρ_c^0 (Table 1), we calculate the (ρ/ρ_c^0) data versus X and Y . The data (64000 points) for all samples collapse close to a single surface in the $(X, Y, \rho/\rho_c^0)$ space. To model the surface analytically, we use $\mathcal{R}(X, Y) = \rho_c^0 \exp[f_1(X)]f_2(Y)$ and fit the functions $f_{1,2}$ with five adjustable parameters as $f_1 = -X + 0.07X^2 + 0.001X^3$ and $f_2 = (1 - Y + 1.48Y^2)/(1 + 1.88Y^2 + 1.72Y^3)$. This procedure yields an agreement of the model surface with the data within 4% rms in the range $|X| \leq 5$ and $Y \leq 3$. The X^2 term in f_1 describes the violation of the reflection symmetry for large X . The analysis of our $\rho(T)/\rho_c(T)$ data confirms that the reflection symmetry $X \leftrightarrow -X$ holds within 0.8% accuracy in the region $|X| < 0.5$, $Y < 0.7$ (see Fig. 3).

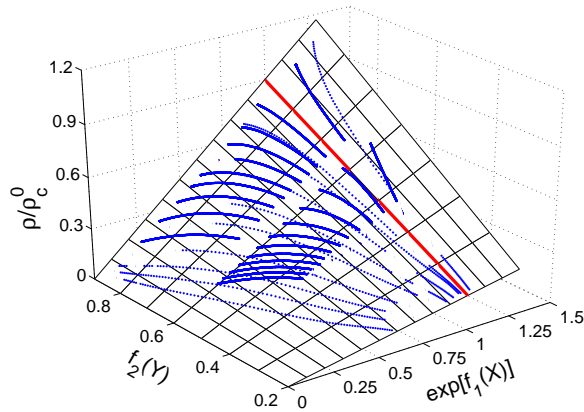


FIG. 4: The empirical two-parameter scaling function $\mathcal{R}(X, Y)$ for five samples (dots) and the model surface $\mathcal{F} = \tilde{X}\tilde{Y}$ (grid). The straight line $\rho/\rho_c^0 = \tilde{Y}$ at $\tilde{X} = 0$ represents the separatrix.

The resulting model surface $\mathcal{F} = \tilde{X}\tilde{Y}$ is plotted in Fig. 4 as a function of $\tilde{X} = \exp[f_1(X)]$ and $\tilde{Y} = f_2(Y)$ together with the scaled data $\rho(T, n)/\rho_c^0$. The data are very close to the model surface; the maximal deviation of the data from the model surface in the ρ direction does not exceed $0.05\rho_c^0$. Clearly, the surface is curved in the both directions. The separatrix $\rho_c(T)$ is represented by the straight line on the model surface (Fig. 4).

In summary, we have performed a detailed two-parameter scaling analysis of the $\rho(T, n)$ data for five Si-MOS samples in the vicinity of the 2D metal-insulator transition. The two-parameter scaling function, which we

have determined experimentally, naturally incorporates the temperature dependence of the separatrix $\rho_c(T)$, the generalized mirror reflection symmetry with respect to $\rho_c(T)$, and the existence of the maximum and inflection points for the $\rho(T)$ dependence on the metallic side. Our analysis strongly supports the interpretation of the critical behavior observed in the transport data as the manifestation of the quantum phase transition driven by both disorder and interaction. The sample to sample variations observed in the exponents κ and ζ , and in the critical resistivity ρ_c^0 value require a quest for new samples in which a random potential will have much shorter correlation length and the inhomogeneities of the electron density will be reduced.

The authors are grateful to A.M.M. Pruisken and A. M. Finkelstein for discussions. The work was supported in part by the RFBR, Programs of RAS, Russian Ministry for Education and Science, Program “The State Support of the Leading Scientific Schools”, Russian Science Support Foundation (D.A.K.), CRDF, FASI, and Dynasty Foundation (I.S.B.).

-
- [1] S. V. Kravchenko *et al.*, Phys. Rev. B **50**, 8039 (1994).
 - [2] S. V. Kravchenko *et al.*, Phys. Rev. B **51**, 7038 (1995).
 - [3] for a review, see S. V. Kravchenko and M. P. Sarachik, Rep. Prog. Phys. **67**, 1 (2004).
 - [4] A. M. Finkelstein, Sov. Sci. Reviews **14**, ed. by I. M. Khalatnikov, Harwood Ac. Publishers, London, (1990), p.3.
 - [5] A. Punnoose, A. M. Finkelstein, Science **310**, 289 (2005).
 - [6] S. Anissimova *et al.*, Nature Phys. **3**, 707 (2007).
 - [7] D. A. Knyazev *et al.*, JETP Lett. **84**, 662 (2006).
 - [8] D. Simonian, S. V. Kravchenko, and M. P. Sarachik, Phys. Rev. B **55**, R13 421 (1997).
 - [9] The absolute values for the carrier density specified in the paper are determined from the period of the quantum magnetooscillations within 1% error, including the vicinity of n_c [10]. The relative deviation in the density $\Delta n/n_c$ is controlled much more precisely, within 0.1%, from the reproducibility of the $\rho(n)$ data for a fixed T .
 - [10] V. M. Pudalov, M. Gershenson, and H. Kojima, in: *Fundamental Problems of Mesoscopic Physics. Interaction and Decoherence*, ed. by I. V. Lerner, B. L. Altshuler, and Y. Gefen, (Kluwer Ac. Publish., Dordrecht, 2004), p. 309.
 - [11] V. Dobrosavljević *et al.*, Phys. Rev. Lett. **79**, 455 (1997).
 - [12] V. M. Pudalov *et al.*, JETP Lett. **68**, 442 (1998); V. M. Pudalov *et al.*, Physica E **3**, 79 (1998).
 - [13] C. Castellani *et al.*, Phys. Rev. B **30**, 527 (1984).
 - [14] See e.g., Chapter 8, p. 212 in D.J. Amit, *Field theory, renormalization group, and critical phenomena*, (World Scientific, 1984).
 - [15] A. de Visser *et al.*, J. Phys.: Conf. Ser. **51**, 379 (2006); A. M. M. Pruisken *et al.*, Sol. State Comm. **137**, 540 (2006).
 - [16] A. M. M. Pruisken, B. Škorić, and M. A. Baranov, Phys. Rev. B **60**, 16838 (1999).
 - [17] W. Li *et al.*, Phys. Rev. Lett. **94**, 206807 (2005).
 - [18] B. Karmakar *et al.*, Physica E **24**, 187 (2004).